

# A microscopic investigation of bubble formation nuclei

D. E. Yount, E. W. Gillary, and D. C. Hoffman

*Department of Physics and Astronomy, and Department of Physiology, University of Hawaii, Honolulu, Hawaii 96822*

(Received 16 January 1984; accepted for publication 14 May 1984)

Numerous experiments suggest that bubble formation in aqueous media is initiated by stable gas nuclei. Although attempts have been made both to detect and to describe these entities, their very existence is still controversial. This paper reports a detailed investigation using light and electron microscopes. The objects identified as nuclei are found in both distilled water and gelatin, and they resemble ordinary gas bubbles. Radii are on the order of  $1\ \mu\text{m}$  or less and can be three orders of magnitude smaller. The number density decreases exponentially with increasing radius. A gas filling is implied by the observation that nuclei expand when the pressure decreases and contract when it rises. The occurrence of nuclear clusters and of binary or osculating nuclei suggests that stabilization is achieved via surfactant films. The monolayer thickness of these films, estimated from the thicknesses of bilayer septa, is  $(20 \pm 7)\ \text{\AA}$ . Many nuclei are embedded in reservoirs of surface-active material made visible by osmium-tetroxide staining. Electron microscope sections are hardened by infiltrating gelatin with epoxy. Reservoirs, encased in epoxy, form microbubble chambers in which the coalescence and bursting of nuclei can be studied during extended exposures to the electron beam.

PACS numbers: 43.25.Yw

## INTRODUCTION

Theoretical calculations of the tensile strength of "pure" or "homogeneous" water give values on the order of 1000 atm, yet ordinary samples of sea water, tap water, or even distilled water form visible bubbles when subjected to tensile, ultrasonic, or supersaturation pressures as small as 1 atm.<sup>1</sup> Similar statements can be made about blood or tissue. If, for example, deep-sea divers exhibited pure water thresholds, they would be free from decompression sickness (the bends) for depths up to 10 km.

The thousandfold discrepancy between homogeneous nucleation theory and experiment is usually explained by saying that the substances in question are "impure" and contain "nuclei" which lower cavitation thresholds.<sup>1</sup> Conversely, thresholds greater than 10 to 100 atm have been measured only by "denucleating" samples or by making them so small that the inclusion of a nucleus becomes unlikely.<sup>2-4</sup> The stability of nuclei can be deduced from the fact that once a liquid has been denucleated, it remains so for extended periods.<sup>5,6</sup> If nuclei are not readily replaced, then those which were originally present in the liquid must have been there a long time. A gas filling is implied by the observations that bubble formation thresholds can be significantly raised by degassing or by a preliminary application of static pressure.<sup>5,6</sup> Solid or liquid nuclei, containing no gas and being essentially incompressible, would not be affected.

The existence of stable gas nuclei is paradoxical. Gas phases larger than  $1\ \mu\text{m}$  in radius should float to the surface of a standing liquid, while smaller ones should dissolve within a few seconds due to surface tension.<sup>7</sup> In a liquid supersaturated with gas, there is one radius at which a bubble would be in equilibrium. However, as was emphasized by Gibbs,<sup>8</sup> even this equilibrium state is unstable. Bubbles larger than

the equilibrium size are expected to grow even larger, while those smaller than the equilibrium size should collapse completely.

In Refs. 9 and 10, the earlier proposals for stabilizing gas nuclei are critically reviewed, and a new model, called the varying-permeability or VP model, is introduced. The essence of the new model is that cavitation nuclei consist of spherical gas phases that are small enough to remain in solution and strong enough to resist collapse, their mechanical compression strength being provided by elastic skins or membranes composed of surface-active molecules. Surface-active molecules are also assumed to be stored in a "reservoir" located just outside the skin, and they can be recruited by the skin in situations where the nucleus expands. Ordinarily, VP skins are gas permeable, but they can become effectively impermeable when subjected to large compressions, typically exceeding 8 atm.

It follows from these assumptions that VP nuclei are remarkably stable. Unlike ordinary gas bubbles, VP nuclei of widely different radii can be stabilized at the same ambient pressure. Under most circumstances, all of the VP nuclei in a sample will have the same internal gas pressure, which is determined by diffusion equilibrium with the surrounding medium. Finally, VP nuclei can be cycled and restabilized at two or more different pressures, providing only that the threshold for bubble formation is not exceeded. This threshold, derived from the Laplace-Young equation, is the same as the condition for an ordinary gas bubble to grow spontaneously,

$$p_{ss} > 2\gamma/r, \quad (1)$$

where

$$p_{ss} \equiv p - p_{amb} \quad (2)$$

is the supersaturation pressure,  $\tau$  is the dissolved gas tension,  $p_{amb}$  is the ambient pressure,  $\gamma$  is the surface tension, and  $r$  is the radius.

The VP model was developed<sup>9,10</sup> because other nucleation mechanisms available at that time appeared to be inconsistent with the data obtained in a comprehensive series of bubble-counting experiments carried out in supersaturated gelatin.<sup>6</sup> By tracking the changes in nuclear radius that are caused by increases or decreases in ambient pressure, the VP model provided a precise quantitative description of these original data<sup>6</sup> and also of the results obtained in various follow-up experiments.<sup>11,12</sup> The model has also been used to calculate diving tables<sup>13,14</sup> and to trace levels of incidence for decompression sickness in a variety of animal species, including salmon, rats, and humans.<sup>15,16</sup>

In the investigation<sup>11</sup> which comes closest to the one reported here, the primitive size distribution of the objects that facilitate bubble formation in gelatin was systematically altered by passing test samples through Nuclepore filters with uniform pore radii of 0.18, 0.27, 0.36, 0.45, and 1.35

$\mu\text{m}$ , accurate to better than  $\pm 10\%$ . From these measurements, it was concluded that the radii calculated in the VP model are those of actual physical structures capable of initiating bubble formation.<sup>11</sup> As in other gelatin experiments,<sup>6,10,12</sup> the number density of the nucleating entities was found to decrease exponentially with increasing radius,<sup>11</sup> a result that has recently been derived theoretically.<sup>17</sup> Because it had previously been shown<sup>6</sup> that the great majority of the bubbles which form in Knox gelatin are associated with the water, rather than with the mixing or the gelatin crystals, it was assumed that the salient properties of nuclei deduced from the gelatin experiments must be characteristic also of nuclei in water and in aqueous media generally.

Finally, mention should be made of the remarkable experiment of Johnson and Cooke,<sup>18</sup> who injected air bubbles into sea water and observed that, although some bubbles dissolved completely, others stopped decreasing in size abruptly and remained as microbubbles apparently stabilized by films. Originally, the radial size distribution ranged up to  $7 \mu\text{m}$  and peaked at around  $2 \mu\text{m}$ . During the first 4 h, there

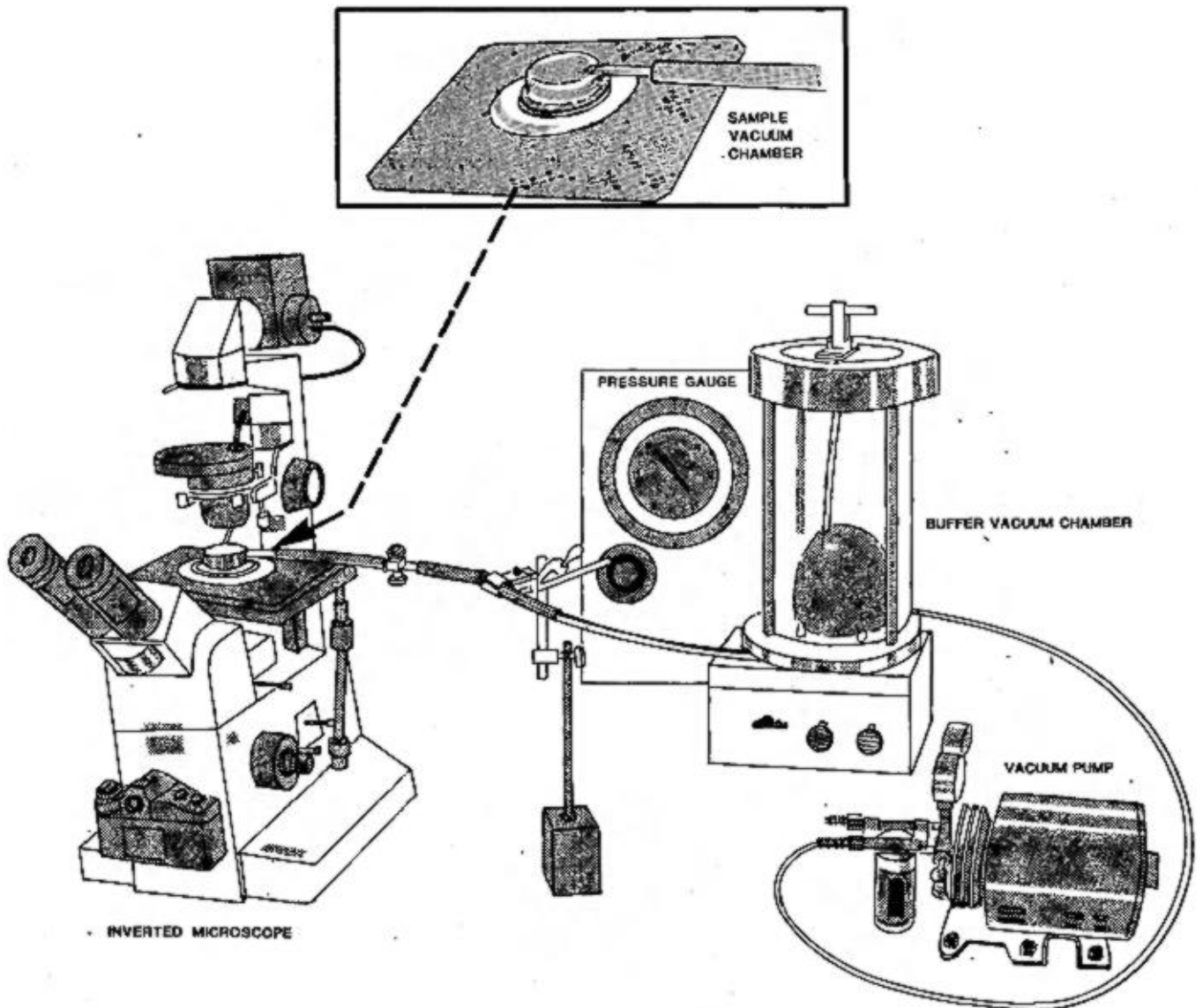


FIG. 1. Inverted phase-contrast microscope and associated vacuum apparatus. With this setup, liquid samples containing nuclear candidates could be subjected to pressures in the range from 0.2 to 1.0 atm abs.

was little change in this distribution. After 22 h, although there was little reduction in the number, the microbubbles were generally smaller, and the radial distribution resembled a decaying exponential, cut off at the microscope resolution, about  $0.3 \mu\text{m}$ . A plausible interpretation of these results is that Johnson and Cooke witnessed the production and stabilization of VP nuclei in sea water.

## I. MATERIALS AND METHODS

The central theme of the above introduction is that aqueous media, in general, and Knox gelatin, in particular, contain a profusion of spherical gas nuclei with radii on the order of  $1 \mu\text{m}$  or less. This fundamental proposition is not universally accepted, and the purpose of the present series of experiments was to test it visually, using both light and transmission-electron microscopes. Preliminary results have been reported already at scientific meetings,<sup>19,20</sup> and a detailed account is given here.

To obtain as much information as possible about the objects being viewed, a variety of microscopes and techniques were tried. Phase-contrast light microscopes proved to be especially sensitive to nuclei because gas inclusions of any type produce large changes in refractive index and, hence, in the relative optical path lengths of the "direct" and "scattered" beams. The use of Nomarsky or interference-contrast optics enhances the perceptions of depth and three dimensionality. Dark-field illumination, in which light is scattered at oblique angles by nuclei, is also quite sensitive and produces images that are virtually free of any background objects or structures. Ordinary bright-field illumination is also feasible, but it is not optimal since nuclei and their surrounding media are both rendered transparent and the contrast is poor. Transmission-electron microscopes are more susceptible to artifacts and distortion, but they permit high resolution and can be used to examine individual nuclei in detail.

The original scanning protocol was to look for structures of any type which appeared to be gas filled or to be associated with a gas phase. Most of the scanning and all of the photography were done by a professional microscopist, the second author, who had no previous knowledge of nucleation models and was therefore relatively unbiased as well as highly trained. The microscopist was also encouraged to photograph and report any unusual objects or phenomena which she might come across. The data collected in accordance with this second protocol proved to be some of the most interesting.

A crucial step in this investigation was the verification that entities of the type identified as "stable gas nuclei" were both stable and gas filled. Much of the evidence for this was obtained with the apparatus shown schematically in Fig. 1. The key element was an inverted phase-contrast microscope, which permitted liquid samples resting on a thin glass plate just above the field lens to remain undisturbed and in focus when subjected to a partial vacuum. The glass vacuum chamber surrounding the sample was connected to a much larger "buffer vacuum chamber" and then to a small vacuum pump. With this setup, pressures in the range from 0.2 to 1.0 atm abs could be applied to the samples within a few seconds.

Nuclear candidates were observed in distilled water and in both Knox<sup>6,11,12</sup> and agarose<sup>21</sup> gelatin. Samples were ordinarily in prolonged contact with air; hence, the dissolved gas tension  $\tau$  was essentially 1 atm abs, as expected from Henry's law. For liquid samples subjected to changes in external pressure using the apparatus shown in Fig. 1, there were two distinctly different situations. In the first, a  $2.5 \times 2.5$ -cm coverslip was placed on top of the sample so that the paths for diffusion from the central viewing region to the edges of the coverslip were long. In this case,  $\tau$  was expected to remain nearly equal to its value at the start of the experiment, 1 atm abs. In the second situation, no coverslip was used, implying that the paths for diffusion from the viewing volume to the upper surface of the sample were short, typically a few tens of microns. In this second case, the dissolved gas tension was expected to equilibrate in less than 1 s with whatever pressure was applied to the surrounding sample vacuum chamber.

Surprisingly, the exact values of the dissolved gas tension have little bearing on the conclusions reached in these experiments. As mentioned in the Introduction, nuclei of the type envisioned in the VP model can be stabilized over a wide range of dissolved gas tensions, ambient pressures, temperatures, and radii, and it is precisely this fact—this remarkable stability—that distinguishes nuclei from ordinary gas bubbles.

Many of the results of this paper were obtained from thin slices of agarose gelatin.<sup>21</sup> Knox or other household gelatins<sup>6,11,12</sup> have the disadvantage that they become moldy after a few days and, hence, cannot be conveniently dried and sectioned. Rigid sections were a necessity in the technique used to prepare electron micrographs, and, although the nuclei seen in water and in fresh Knox or agarose gelatin with light microscopes resembled those identified in dried sections of agarose, their rapid motion often made it difficult to obtain clear micrographs in these substances. Finally, the number densities in agarose were some five orders of magnitude higher than in typical samples of distilled water, while those in water were another one or two orders of magnitude higher than in Knox gelatin. As a result of these enormous differences, the scanning time required to find a nucleus was ordinarily several hours in Knox gelatin and up to 1 h in water, whereas every agarose sample or section yielded success within a few minutes.

The first step in preparing agarose thin sections was to enhance the stiffness of the test material by "saturating" the sol with agarose powder, that is, by dissolving as much powder as possible before allowing the sol to cool. Agarose samples to be sectioned for the phase-contrast, Nomarsky, dark-field, and bright-field microscopes were allowed to dry out at room temperature for several days. This further increased the stiffness and reduced the water concentration from about 95% to 85% w/w. Sections  $2.5 \mu\text{m}$  thick were then cut, and no auxiliary processing, such as fixing or staining, was required. Samples destined for the transmission-electron microscope, on the other hand, were subjected to a routine procedure normally applied to animal tissue. This included fixing in glutaraldehyde, staining in osmium tetroxide, dehydration with ethanol, and a final infiltration of the sample

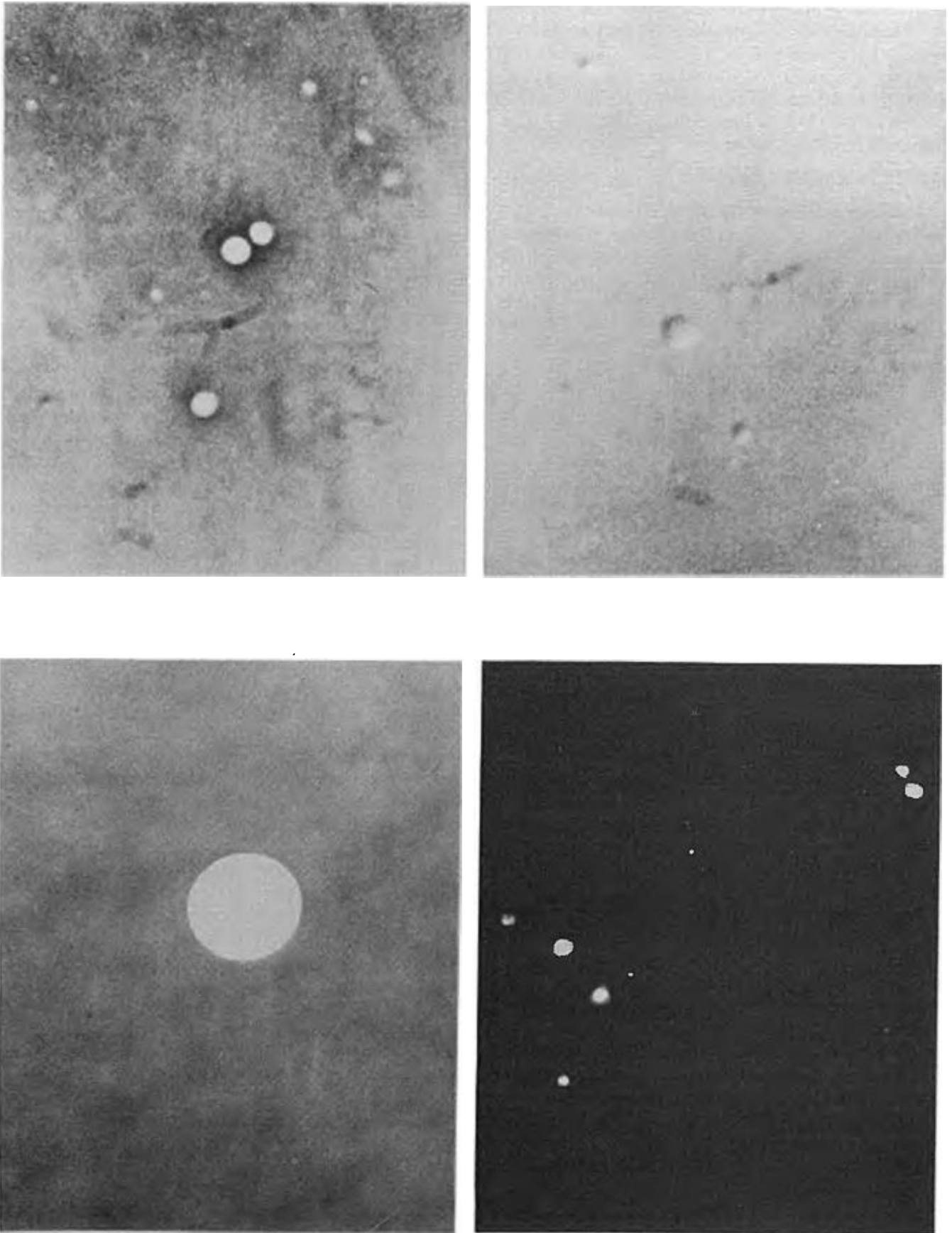


FIG. 2. Photomontage of candidate nuclei found in agarose. Moving clockwise from upper left are phase-contrast, Nomarsky, dark-field, and transmission-electron micrographs. The largest nuclei in each case have radii on the order of  $1\ \mu\text{m}$ .

with epoxy resin. Sections of the desired thickness, typically  $0.09\ \mu\text{m}$ , were cut from hardened epoxy blocks using a diamond knife.

One of the outcomes of the microscope experiments was the accidental discovery of a method by which certain interactions and dynamical properties of bubble-formation nuclei can be investigated. The method is particularly promising because it can be applied quite easily to objects or structures as small as a few tens of angstroms. The general observation is that beams of light or of electrons can be used to heat samples containing nuclei while they are being viewed. In the case of the liquid samples seen with light microscopes, the results are rather chaotic, and it is difficult to track heated nuclei, let alone photograph them. Dried samples studied with light microscopes show very little effect. In the case of hardened samples viewed with the transmission-electron microscope, however, the nuclei and their surrounding reservoirs are perforce trapped in epoxy thin sections, which serve not only to hold them in place, but also to constrain the total volume, the shape, and the material content. The confined volumes and their epoxy walls are referred to in this paper as "microbubble chambers." Within these chambers, some truly remarkable phenomena have been observed.

## II. RESULTS

Nuclear candidates seen in water and fresh gelatin "squashed" between a coverslip and a glass microscope slide exhibit Brownian motion and are usually in rapid translation. In some cases, it has been possible to follow a particular

candidate for several minutes, thereby demonstrating its stability and a persistence time that is at least two orders of magnitude longer than the theoretical dissolution time for an ordinary gas bubble.<sup>7</sup>

A photomontage of candidate nuclei found in thin sections of agarose gelatin is shown in Fig. 2. Moving clockwise from upper left are phase-contrast, Nomarsky, dark-field, and transmission-electron micrographs. The structures identified as nuclei with phase-contrast and Nomarsky optics resemble ordinary gas bubbles. In the Nomarsky micrograph, the shadowing of the nuclei is opposite that of the surrounding gelatin, implying that nuclei are spherical cavities, rather than solid or liquid inclusions. Nuclei seen with dark-field illumination often have halos and are reminiscent of planetary systems, such as the moons of Jupiter. Large nuclei detected with the transmission-electron microscope usually appear as circular or ellipsoidal holes with clean edges. In all cases, the size distributions and shapes are similar, and there are few, if any, background constituents. Under these circumstances, it is reasonable to assume that the same kind of object is being observed by all of the microscope techniques and in distilled water as well as in Knox and agarose gelatin.

Near the center of the phase-contrast micrograph in Fig. 2 are two osculating nuclei, that is, two nuclei which are

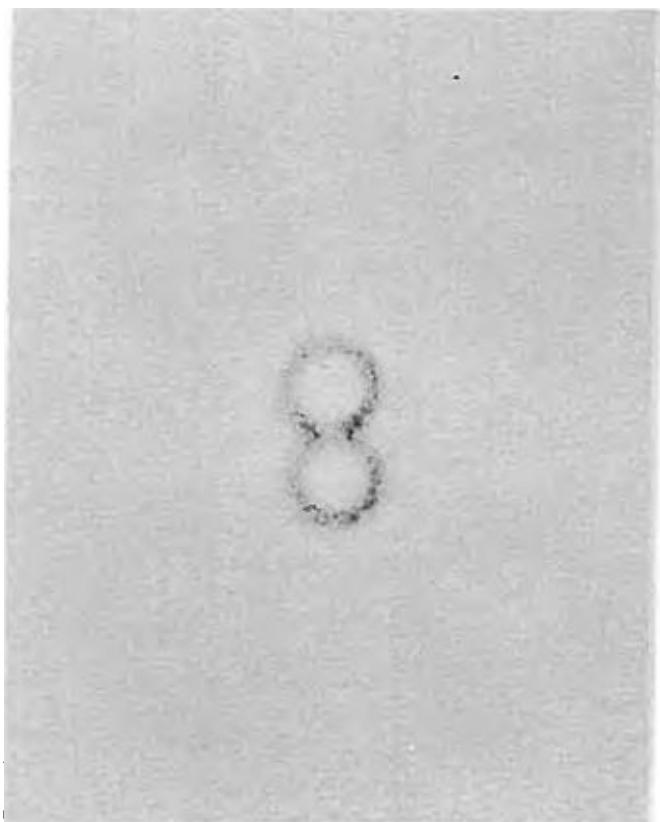


FIG. 3. Two osculating nuclei photographed in distilled water with ordinary bright-field illumination. The larger member of this stable binary has a radius of  $1.5\ \mu\text{m}$ .

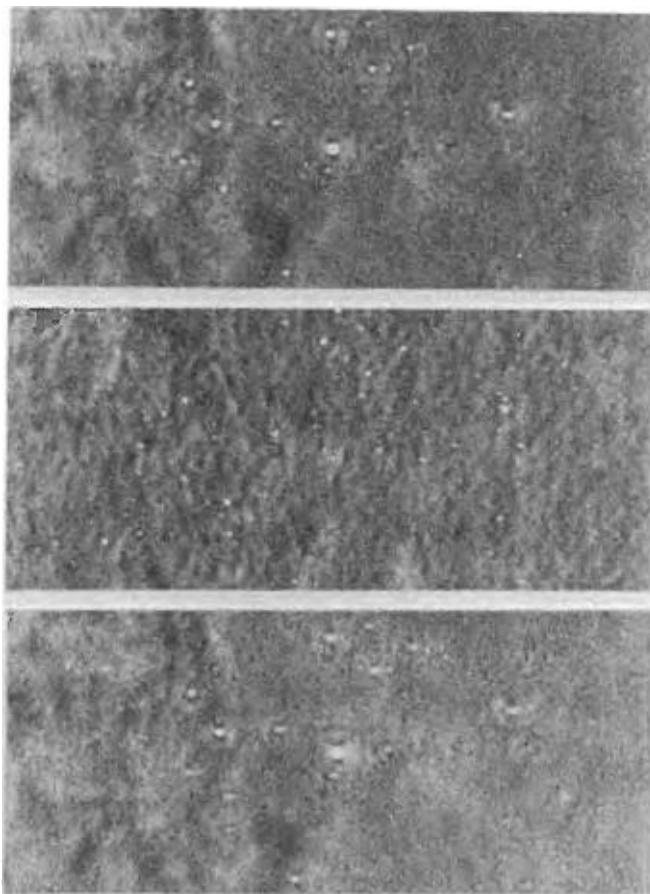


FIG. 4. Results of a "vacuum-on, vacuum-off" experiment carried out with the apparatus shown in Fig. 1. The upper and lower micrographs were taken at  $0.26\ \text{atm abs}$ , and the one in the center was taken at  $1.00\ \text{atm abs}$ . The main conclusion is that nuclei expand when the pressure falls and contract when it rises. It follows that they must be gas filled. A second conclusion is that nuclei can be stabilized at different radii and pressures.

just barely touching and appear still to be spherical at the point of contact. In agarose, about 5% of the identified structures are of this type. Binary systems have also been seen in distilled water. One example, photographed with ordinary bright-field illumination, is shown in Fig. 3. Although the contrast is poor, the observation of osculating nuclei in water is important because it demonstrates that complex structures such as these are not artifacts associated only with the use of gelatin, the preparation of thin sections, etc.

The results of a "vacuum-on, vacuum-off" experiment performed with liquid agarose under a coverslip are summarized in Fig. 4. Although the magnification and resolution of the inverted phase-contrast microscope depicted in Fig. 1 are lower than those of the high-quality phase-contrast microscope referred to in Fig. 2, the number densities, physical sizes, and general appearances of the candidate nuclei are the same. The upper and lower micrographs in Fig. 4 were taken at 0.26 atm abs, and the middle photograph was taken at 1.00 atm abs. The main conclusion from this study is that nuclei expand when the pressure falls and contract when it rises. Since solid or liquid nuclei would be insensitive to such changes in pressures, the objects being investigated must be gas filled. A second conclusion from the "vacuum-on, vacuum-off" experiment is that bubble formation nuclei are very stable. The three micrographs shown in Fig. 4 are part of a longer sequence demonstrating that nuclei can be cycled repeatedly and still survive. Not only are nuclei of different radii stable at the same pressure setting, but a given nucleus can be restabilized at two or more different pres-

ures, provided that the threshold for bubble formation is not exceeded. There was a tendency for some of the objects seen in Fig. 4 to drift out of focus as the series progressed. Most of the candidates, however, could be tracked from beginning to end.

When the "vacuum-on, vacuum-off" experiment was repeated without a coverslip, the results were very different. During the initial decompression, candidate nuclei became smaller, rather than larger, and some of them could no longer be seen. During the subsequent compression, nuclei were neither regenerated nor restored. This sequence is a direct demonstration of the well-known technique for denucleating samples by degassing.<sup>5</sup> The time required for both degassing and denucleation was short because the samples were so thin.

Figure 5 is a sequence of electron micrographs taken during a 4 min exposure of one portion of an agarose thin section to the electron beam. At first, binary or trinary microbubble systems can be seen embedded in each of the three regions darkened by osmium-tetroxide staining. Because osmium is normally used to increase the contrast of surface-active materials, including cell membranes, it is reasonable to assume that the darkened regions are rich in surfactants and tentatively identify them as the nuclear "reservoirs" postulated in the VP model.<sup>10,17</sup> A related assumption is that these reservoirs and the nuclei embedded in them were present in the original agarose sample and remained intact throughout the fixing, staining, dehydration, and infiltration required to produce thin sections for the electron microscope.

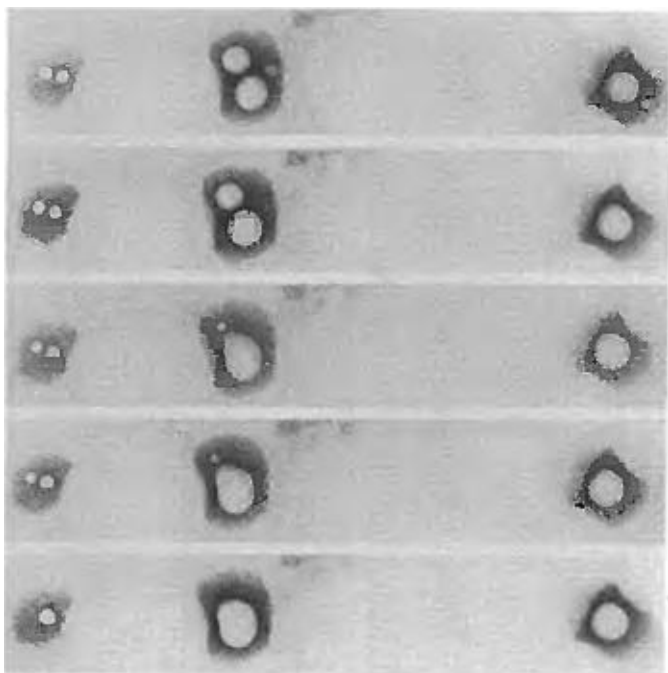


FIG. 5. Sequence of five electron micrographs taken during a 4 min exposure to the electron beam. Osculating nuclei can be seen embedded in each of three "reservoirs" darkened by osmium-tetroxide staining. As this portion of the agarose thin section is warmed by the electron beam, the respective microbubble systems coalesce to form one gas phase per reservoir. In this case, coalescence occurs via diffusion of gas through the nuclear skins, which appear as dark borders or outlines and which at all times remain intact. The radius of the largest nucleus in the first micrograph is  $0.03 \mu\text{m}$ .

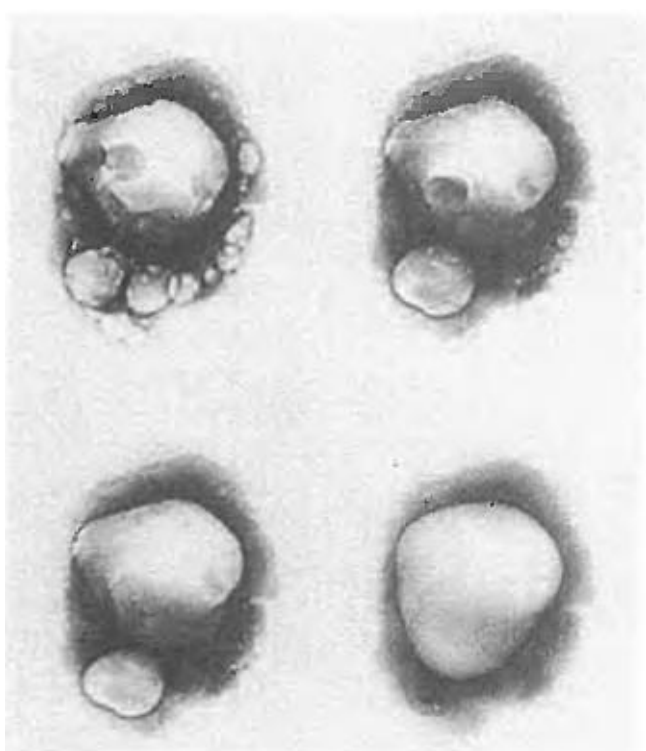


FIG. 6. Time progression of a nuclear cluster exposed for several minutes to the electron beam. The end result is again a single gas phase embedded in a reservoir. The reservoir is encased in hardened epoxy, which is airtight and prevents the gas phase from becoming truly spherical. The largest gas-phase diameter visible in the final micrograph is  $0.13 \mu\text{m}$ .



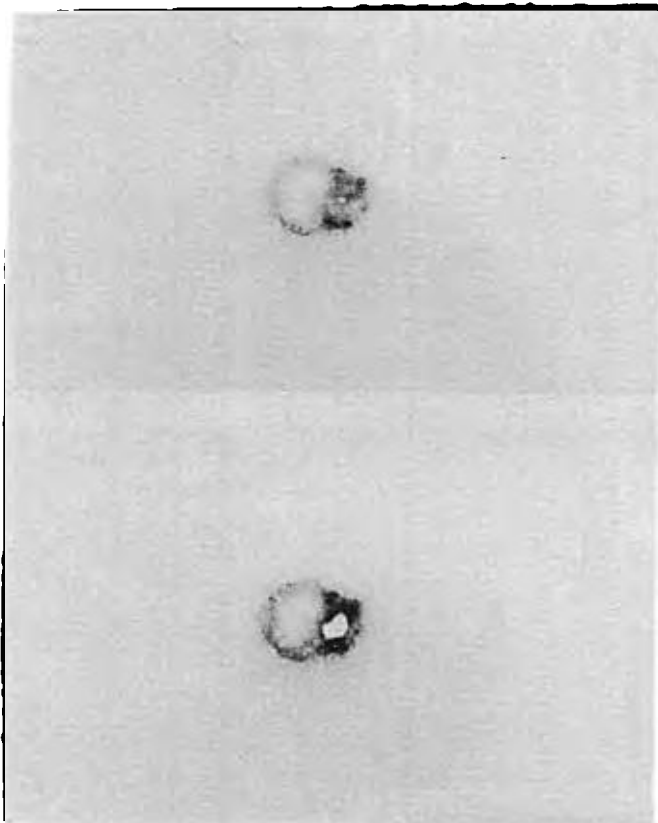


FIG. 7. Example of a microbubble system which "pops" when heated sufficiently by the electron beam. The upper micrograph was taken just before and the lower just after popping occurred. Popping releases a burst of gas which can momentarily shut off the electron beam. The radius of the spherical portion of this object is  $0.3 \mu\text{m}$ .

The reservoirs in Fig. 5 are completely encased in airtight, hardened epoxy, thereby forming three separate "microbubble chambers." As this portion of the agarose thin section is warmed by the electron beam, the contents of the microbubble chambers seem to melt, allowing the enclosed nuclei to coalesce and form one gas phase per reservoir. In this case, coalescence occurs via diffusion of gas through the nuclear skins, which appear as dark borders or outlines and which at all times remain intact. As one might expect from the behavior of ordinary soap bubbles, smaller microbubbles discharge their contents into larger ones. This is another consequence of the Laplace-Young equation, which associates a pressure difference  $\Delta p = 2\gamma/r$  with a surface tension  $\gamma$  and radius of curvature  $r$ .

Figure 6 shows the time progression of a nuclear cluster exposed for several minutes to the electron beam. Such clusters account for approximately 2% of the candidate structures found in agarose, but none have yet been seen in distilled water. As in Fig. 5, the membranes surrounding the individual gas compartments are clearly visible. The end result of this exposure is again a single spheroidal gas phase embedded in a reservoir.

The outer boundaries of the reservoirs in Figs. 5 and 6 are not noticeably altered by the beam. Evidently, the walls of the respective microbubble chambers are fairly rigid and

melt at a temperature that is relatively high. In two instances, however, the beam has heated a chamber to the point where an encased microbubble "pops" through the epoxy wall and releases a burst of gas which, although minute, is sufficient momentarily to shut off the beam. The photographic record of one of these events is shown in Fig. 7, providing additional evidence that the objects being studied are gas filled and remain so throughout fixing, staining, dehydration, infiltration, and sectioning.

Theoretically, there is no stable configuration of aggregating bubbles inside a homogeneous liquid which involves a shared boundary layer or membrane.<sup>22</sup> The osculating nuclei seen in Figs. 2 and 3, for example, are just barely touching. Within a rigid microbubble chamber, however, common septa and a foamlike microbubble structure are possible. This is illustrated in Fig. 8, which contains a number of gas-filled compartments and many shared membranes. The latter have a tendency to intersect at  $120^\circ$ , as expected from Plateau's rules.<sup>23</sup> When this section is heated with the electron beam, coalescence occurs via the breaking of shared membranes as well as by diffusion through membranes that remain intact.

Figure 9 shows a nucleus encumbered by solid (i.e., opaque) debris. The radius of the nucleus itself is about  $1.0 \mu\text{m}$ , and surface contaminants are detectable down to a few tens of angstroms. Figure 9 also contains an intact septum and what appear to be the remnants of a much larger septum which may have ruptured during sectioning. Because shared membranes or septa by themselves are intrinsically unstable,<sup>22</sup> as already mentioned, it is probably no accident that those seen in this micrograph are bordered by solid particles. The assumption is once again being made that this entire microbubble structure, including gas compartments, septa, and attached particles, was present in a similar form in the original agarose sample.

The differential radial distribution of gas cavitation nuclei in agarose is plotted in Fig. 10. These data were obtained with the high-resolution phase-contrast microscope referred to in Fig. 2. The scanning efficiency deteriorates rapidly below  $0.2 \mu\text{m}$ , and points in this region should be disregarded. Above  $0.2 \mu\text{m}$ , the measurements can be described by a decaying exponential. The  $\chi^2$  for 13 bins (including the bin from  $1.400$  to  $1.499 \mu\text{m}$  with  $N = 0$ ) and 11 degrees of freedom is 11.6. The exponential radial distribution is a signature for gas cavitation nuclei, as previously noted.<sup>6,10-12,17</sup> An estimate of the total number density can be obtained by extrapolating the exponential to zero radius. The result is  $10^{10}$  nuclei/cm<sup>3</sup>. The number density is five orders of magnitude lower in local samples of distilled water and six or seven orders of magnitude lower in typical samples of Knox gelatin.

### III. DISCUSSION

Previous experiments with Knox gelatin have demonstrated that, although some nuclei are definitely associated with the gelatin crystals, the great majority were present already in the distilled water used in mixing.<sup>6,11,12</sup> Another relevant finding is that some (and perhaps all) specimens of Knox gelatin stock contain substances capable of eliminat-

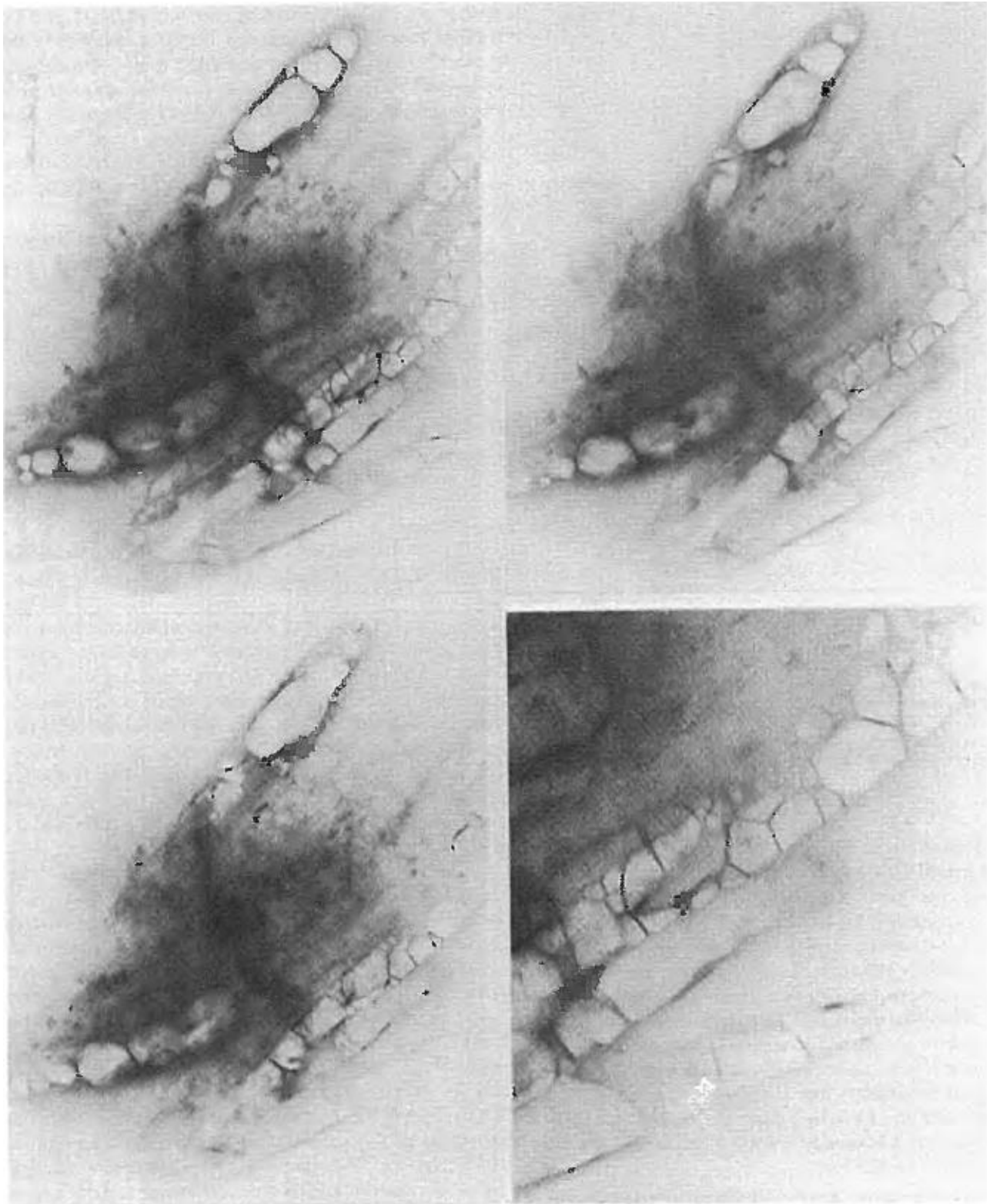


FIG. 8. Irregularly shaped microbubble complex exposed for several minutes to the electron beam. The upper-left, upper-right, and lower-left micrographs were taken in that order, and the lower-right micrograph is an enlargement of the upper-left. The rigid epoxy walls of the "microbubble chamber" encasing this reservoir can support shared membranes, which have a tendency to intersect at  $120^\circ$ . As this section is heated, coalescence proceeds via the breaking of shared membranes as well as by diffusion through membranes that remain intact. The height of the entire configuration is about  $0.8 \mu\text{m}$ .

ing nuclei.<sup>6,11,12</sup> The microscope studies are consistent with these earlier inferences in that: Candidate nuclei were found in both distilled water and Knox gelatin; the number densities were one or two orders of magnitude higher in distilled water than in Knox gelatin; and the number densities in

Knox gelatin were in the range (on the order of  $10^3$  to  $10^4$  nuclei per  $\text{cm}^3$ ) that would be expected from published bubble counts.<sup>6,11,12</sup> In Knox gelatin, therefore, and probably also in distilled water, the correspondence between supercritical nuclei and bubbles appears to be one to one.



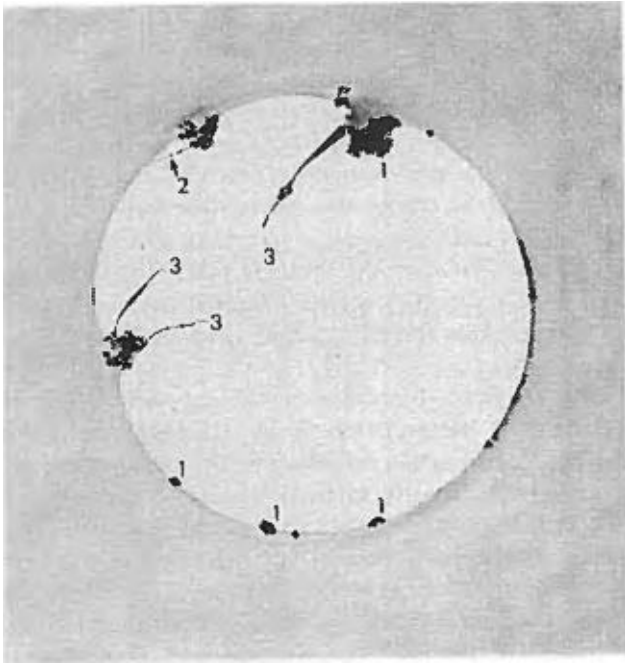


FIG. 9. Nuclear candidate encumbered by solid debris. The radius of the gas phase is about  $1.0\ \mu\text{m}$ , and solid particles (1) accreted at the liquid-gas interface are detectable down to a few tens of angstroms. This specimen also contains an intact septum (2) and the possible remnants (3) of a much larger septum which may have ruptured during sectioning.

A one-to-one correspondence may be viewed in the context of the varying-permeability model<sup>9,10</sup> as a consequence of the "ordering hypothesis" and the "criterion for bubble formation." The former states that nuclei are neither created nor destroyed by a pressure schedule and the initial ordering according to size is preserved. The latter, given by Eq. (1), requires that all nuclei larger than  $2\gamma/p_{ss}$  at the end of the pressure schedule will form macroscopic bubbles. From these two assumptions, it is deduced that every nucleus with initial radius  $r_0$  larger than some minimum critical value  $r_0^{\text{min}}$  will eventually form a gross bubble.<sup>9,10</sup>

The situation in agarose gelatin must be very different. With a number density on the order of  $10^{10}$  per  $\text{cm}^3$ , agarose is "hypernucleated." For every gross bubble that is counted in a typical experiment, there must be a vast number of supercritical nuclei that begin to grow but soon lose out in the severe competition for excess dissolved gas. Neighboring cavities may rob gas from one another or coalesce to form larger and more viable structures.<sup>22</sup> The correspondence between supercritical nuclei and gross bubbles would then no longer be one to one but might be on the order of  $10^7$  to 1. The nuclei themselves<sup>9,10</sup> and their initial exponential size distribution<sup>17</sup> could still be described by the VP model, but their behavior in the "phase-equilibration" regime<sup>24</sup> of agarose gelatin would be unlike that in the "nucleation-limited" regime of Knox gelatin and distilled water. In the phase-equilibration regime, for example, nucleation is so profuse that virtually all of the excess gas comes rapidly out of solution,<sup>24</sup> and the number of bubbles is not determined by nucleation *per se* but by other factors, such as the speed with which supersaturation is induced and the homogeneity and stiffness of the surrounding medium. It is not known why

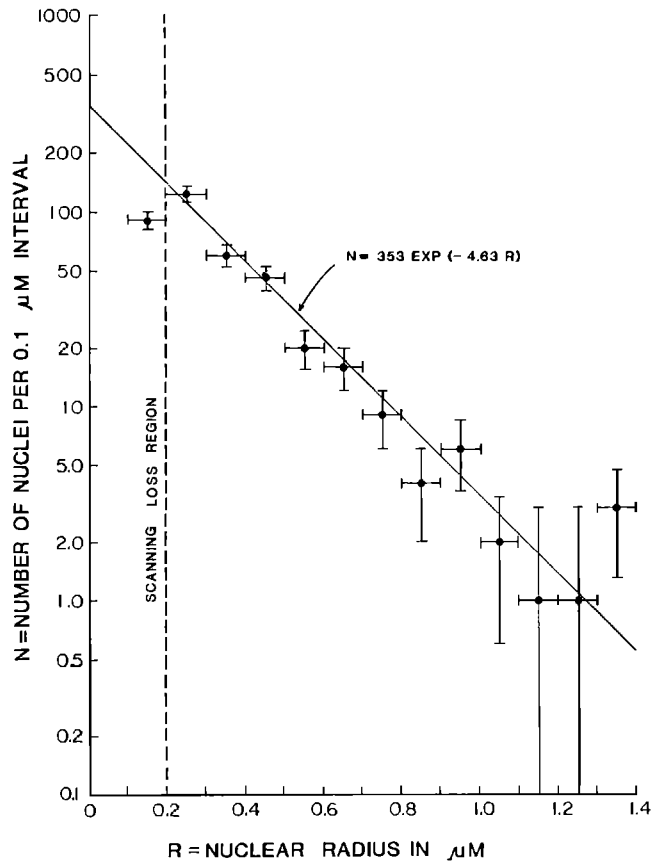


FIG. 10. Differential radial distribution of gas cavitation nuclei in agarose. The scanning efficiency deteriorates rapidly below  $0.2\ \mu\text{m}$ , and data in this region should be disregarded. Above  $0.2\ \mu\text{m}$ , the results can be described by a decaying exponential.

agarose gelatin contains so many nuclei, whether these nuclei are present already in the agarose crystals, or whether the crystals contain substances which are capable of stabilizing cavitation nuclei.

The accretion of solid debris by ordinary gas bubbles has been used for many years to separate mineral ores from gangue by "flotation." This process can be controlled and significantly enhanced by adding appropriate surfactants.<sup>25</sup> Attached particles and surfactant coatings may also account, respectively, for the neutral buoyancy and the long persistence in sea water of microbubbles with radii up to  $60\ \mu\text{m}$ .<sup>26</sup> The "persistent microbubbles" detected in sea water are, of course, much larger than any "cavitation nuclei" reported here. Furthermore, the slope of the exponential distribution plotted in Fig. 10 is too steep to permit an appreciable number of nuclei with radii greater than  $10\ \mu\text{m}$ . These facts can easily be reconciled with the VP model by assuming that persistent microbubbles and cavitation nuclei are indeed the same type of structure and that their characteristic exponentials have different slopes, the slope being a function mainly of the chemistry of the surrounding medium and the binding energy of the respective surfactant molecules to the skin.<sup>10,17</sup> The characteristic exponential is not expected to be manifested in the residual size distribution of persistent microbubbles because this distribution is determined mainly by the spectra of available particles and the neutral-buoyancy requirement.<sup>26</sup>

The tendency of bubble-formation nuclei to accrete solid debris was deduced already from the gelatin filtration experiment and is discussed especially in the two appendices of Ref. 11. Ideally, each filter in that investigation would have eliminated all of the nuclei in the sample with cavitation radii larger than the filter-pore radius and none with cavitation radii that were smaller. In practice, the former condition was satisfied, while the latter was not. It is now evident that there are at least four nucleating systems for which the geometric radius can be larger than the cavitation radius, namely, isolated nuclei encumbered by solid particles, nuclei embedded in extensive reservoirs, osculating nuclei, and nuclear clusters. A fifth example, not encountered in the present study, would be gas-filled crevices in motes.<sup>5</sup>

The thickness of the intact septum in Fig. 9 is  $(49 \pm 14)$  Å. It is plausible that this septum consists of two layers of aligned surfactant molecules separated by a thin liquid channel, as would be the case for a minimal soap film with air on either side.<sup>27</sup> Allowing 10 Å for the channel,<sup>22,27</sup> the estimated thickness of a monolayer or nuclear skin is  $(20 \pm 7)$  Å. Similar but less accurate estimates of the skin thickness can be obtained from the darkened borders in Fig. 5, from the minimum gas-phase separations in Fig. 5 and from the thicknesses of various common septa in Fig. 8. The thicknesses of typical monolayers range from 5 to 50 Å.<sup>28</sup>

With the high-resolution phase-contrast optical microscope, it has been confirmed that the primordial size distribution of bubble formation nuclei in agarose decreases exponentially with increasing radius in the range from 0.2 to 1.5  $\mu\text{m}$ . The ranges covered in previous experiments in Knox gelatin were 0.07 to 0.7  $\mu\text{m}$ ,<sup>6</sup> 0.18 to 1.35  $\mu\text{m}$ ,<sup>11</sup> and 0.007 to 0.17  $\mu\text{m}$ ,<sup>12</sup> respectively. The VP model has been used to calculate the radii of nuclei subjected to high pressures, and values as small as 0.004  $\mu\text{m}$  have been obtained.<sup>12</sup> It is an interesting question whether stable gas phases of this size are physically realizable. Although it should be possible to trace the primordial distribution far below 0.2  $\mu\text{m}$  by using the transmission-electron microscope, this was not attempted because of uncertainties and possible biases in the scanning efficiency. It is important to note, however, that many candidates were found with radii as small as 0.001  $\mu\text{m} = 10$  Å, the limit of the electron microscope resolution. Furthermore, the number density may still be exponential in this region.

The fact that no intrinsic minimum or cutoff has been observed at the 10-Å level suggests that "homogeneous" generation of stable gas nuclei may be feasible in highly concentrated agarose.<sup>1</sup> Such a process could account for the high number density in this medium. Another possible mechanism is that proposed for the *de novo* formation of cylindrical gas vacuoles in blue-green algae.<sup>29</sup> In the limit of zero radius, the VP nucleus would become truly a micelle and not just "a micelle with gas inside."<sup>9</sup>

The findings of this experiment, though sometimes unexpected, appear to be remarkably consistent with the VP model.<sup>9,10,17</sup> The most important point is that nuclear candidates are stable microbubbles, i.e., gas phases that tend to have a spherical shape and are apparently stabilized by elastic skins or membranes consisting of surface-active molecules. Surface-active molecules seem also to collect in reser-

voirs located just outside the skins. Although no reservoirs have been detected in water or gelatin viewed with optical microscopes, they are easy to find in electron micrographs made of agarose samples darkened by osmium-tetroxide staining. Osculating nuclei and nuclear clusters have a simple explanation in the VP model via the tendency of surfactant films to attract one another and form bilayers.<sup>27</sup> In some cases, nuclear clusters consist of numerous spheres floating freely in a shared reservoir, while in other cases, they are crammed together, partitioning a limited space with their shared membranes and filling it with irregularly shaped gas compartments.

The conditions for coalescence appear also to be consistent with a VP interpretation. Since VP skins are ordinarily permeable to gas, nuclei embedded in the same medium will normally have the same internal pressure, independent of their radii. The smaller of the two osculating nuclei in Fig. 3 does not discharge its contents into the larger, as would be the case for ordinary gas bubbles, because the diffusion gradient across their skins is zero. This is made possible in the VP model<sup>9,10,17</sup> by the "skin compression"  $\Gamma$ , which can vary from zero up to maximum value  $\gamma_C$ . In the case shown in Fig. 3,  $\Gamma$  exactly cancels the normal interfacial tension  $\gamma$ , thereby yielding a net surface tension  $\gamma' = \gamma - \Gamma$ , which is zero. Warming is expected to decrease  $\gamma_C$  as the surfactant molecules become less tightly bound. When  $\gamma_C$  falls below  $\gamma$ , as in Figs. 5, 6, and 8, the skin compression is no longer able to neutralize the interfacial tension completely, and coalescence begins to occur, either via diffusion through nuclear membranes that remain intact or through the breaking of a common septum which allows two adjacent compartments to merge.<sup>22</sup>

Warming also increases the vapor pressure and the pressure of gas already inside a microbubble, and by decreasing the solubility, it causes additional gas to come out of solution. As the pressure inside the microbubble chamber in Fig. 7 rises, the chamber itself "pops," thereby releasing a burst of gas which momentarily shuts off the electron beam. Although the quantity of gas liberated in this process is minute compared to that already present in the entire microscope vacuum chamber, its effect appears to be very much enhanced due to the positioning of the specimen directly in the electron beam. In this configuration, the beam channel upstream of the specimen seems to act like the barrel of a gun, guiding a tiny shock wave of released gas backwards from the specimen to the highly sensitive filament.

The objects studied in this experiment appear to have all of the properties required to initiate bubble formation. Nevertheless, the complete process culminating in a macroscopic bubble has not yet been observed. The explanation for this is clear. In the case of agarose gelatin, only about one nucleus out of ten million is expected to form a gross bubble in a typical case. Nuclei are difficult to find in Knox gelatin, and, in water, expanding nuclei quickly float out of view. A possible method for photographing bubble formation in water would be to trap the growing gas phase on the underside of a glass plate, a technique described in Refs. 18 and 30.

There is considerable evidence that gas-filled crevices can also act as cavitation nuclei.<sup>5,31</sup> The crevice mechanism

is certainly viable,<sup>5</sup> and it is generally believed to be the main factor responsible for bubble formation that occurs on solid surfaces and container walls, a phenomenon that is still under active investigation.<sup>32</sup> Whereas solid particles were occasionally seen in the present microscope experiments, both in isolation and adherence to an interface as in Fig. 9, their role appears to be incidental. In particular, most interfaces are completely free of visible contaminants. When solid particles are associated with a gas phase, they cover only a small fraction of the interfacial area. "Ragged surfaces" are common, as reported in Ref. 33, but none of the crevices seen here in isolated particles were gas filled. This null result carries some weight because crevices examined with the transmission-electron microscope are viewed in cross section, rather than head on as with the scanning electron microscope used in Ref. 33, and there is a reasonable chance of identifying a gas filling if one is present. The final point, therefore, is that gas-filled crevices in motes, if they exist in bulk water or gelatin, are very rare in comparison with their spherical counterparts.

#### ACKNOWLEDGMENTS

It is a pleasure to thank our colleagues Ed Beckman, Ian Cooke, Ruth Kleinfeld, Nancy Lind, Nancy Morrison, Jon Pegg, and Birch Porter for assistance and helpful suggestions. The sample vacuum chamber was designed and fabricated by Bill Cooper. This work, carried out under "The Physics of Gas Bubbles: Medical Applications" Project (HP/R-4), is a result of research sponsored in part by the University of Hawaii Sea Grant College Program under Institutional Grant Number NA81AA-D-00070 from NOAA Office of Sea Grant, U. S. Department of Commerce. This is Sea Grant Publication Number UNIH-SEAGRANT-JC-85-05.

<sup>1</sup>M. Blander and J. L. Katz, *AIChE J.* **21**, 833-848 (1975).

<sup>2</sup>L. J. Briggs, *J. Appl. Phys.* **21**, 721-722 (1950).

- <sup>3</sup>W. A. Gerth and E. A. Hemmingsen, *Z. Naturforsch.* **31A**, 1711-1716 (1976).
- <sup>4</sup>R. E. Apfel, *J. Acoust. Soc. Am.* **49**, 145-155 (1970).
- <sup>5</sup>E. N. Harvey, D. K. Barnes, W. D. McElroy, A. H. Whiteley, D. C. Pease, and K. W. Cooper, *J. Cell. Comp. Physiol.* **24**, 1-22 (1944).
- <sup>6</sup>D. E. Yount and R. H. Strauss, *J. Appl. Phys.* **47**, 5081-5088 (1976).
- <sup>7</sup>P. S. Epstein and M. S. Plesset, *J. Chem. Phys.* **18**, 1505-1509 (1950).
- <sup>8</sup>J. W. Gibbs, *Trans. Conn. Acad.* **3**, 343-520 (1878).
- <sup>9</sup>D. E. Yount, T. D. Kunkle, J. S. D'Arrigo, F. W. Ingle, C. M. Yeung, and E. L. Beckman, *Aviat. Space Environ. Med.* **48**, 185-191 (1977).
- <sup>10</sup>D. E. Yount, *J. Acoust. Soc. Am.* **65**, 1429-1439 (1979).
- <sup>11</sup>D. E. Yount, C. M. Yeung, and F. W. Ingle, *J. Acoust. Soc. Am.* **65**, 1440-1450 (1979).
- <sup>12</sup>D. E. Yount and C. M. Yeung, *J. Acoust. Soc. Am.* **69**, 702-708 (1981).
- <sup>13</sup>D. E. Yount and D. C. Hoffman, *Cavitation and Multiphase Flow Forum 1983*, edited by J. W. Hoyt (*Am. Soc. Mech. Eng.*, New York, 1983), pp. 65-68.
- <sup>14</sup>D. E. Yount and D. C. Hoffman, *Underwater Physiology VIII: Proceedings of the Eighth Symposium on Underwater Physiology*, edited by A. J. Bachrach and M. M. Matzen (*Undersea Med. Soc.*, Bethesda, MD, 1984), pp. 131-146.
- <sup>15</sup>D. E. Yount, *Aviat. Space Environ. Med.* **50**, 44-50 (1979).
- <sup>16</sup>D. E. Yount, *Undersea Biomed. Res.* **8**, 199-208 (1981).
- <sup>17</sup>D. E. Yount, *J. Acoust. Soc. Am.* **71**, 1473-1481 (1982).
- <sup>18</sup>B. D. Johnson and R. C. Cooke, *Science* **213**, 209-211 (1981).
- <sup>19</sup>D. E. Yount, E. W. Gillary, and D. C. Hoffman, *Cavitation and Polyphase Flow Forum 1982*, edited by J. W. Hoyt (*Am. Soc. Mech. Eng.*, New York, 1982), pp. 6-9.
- <sup>20</sup>D. E. Yount, E. W. Gillary, and D. C. Hoffman, *Underwater Physiology VIII: Proceedings of the Eighth Symposium on Underwater Physiology*, edited by A. J. Bachrach and M. M. Matzen (*Undersea Med. Soc.*, Bethesda, MD, 1984), pp. 119-130.
- <sup>21</sup>J. S. D'Arrigo, *Aviat. Space Environ. Med.* **49**, 358-361 (1978).
- <sup>22</sup>D. E. Yount, *J. Colloid Interface Sci.* **91**, 349-360 (1983).
- <sup>23</sup>J. C. C. Nitsche, *Am. Math. Mono.* **81**, 945-968 (1974).
- <sup>24</sup>B. A. Hills, *Int. J. Biometeor.* **14**, 111-131 (1970).
- <sup>25</sup>A. W. Adamson, *Physical Chemistry of Surfaces* (Wiley, New York, 1976), 3rd ed., pp. 459-474.
- <sup>26</sup>P. J. Mulhearn, *J. Geophys. Res.* **86**, 6429-6434 (1981).
- <sup>27</sup>A. S. C. Lawrence, *Soap Films: A Study of Molecular Individuality* (Bell, London, 1929), pp. 28-128.
- <sup>28</sup>G. L. Gaines, Jr., *Insoluble Monolayers at Liquid-Gas Interfaces* (Interscience, New York, 1966), p. 112.
- <sup>29</sup>A. E. Walsby, *Sci. Am.* **237**, 90-97 (1977).
- <sup>30</sup>L. Lieberman, *J. Appl. Phys.* **28**, 205-211 (1957).
- <sup>31</sup>For a recent review of the crevice model, see the article by L. A. Crum, *Appl. Sci. Res.* **38**, 101-115 (1982).
- <sup>32</sup>R. H. S. Winterton, *J. Phys. D: Appl. Phys.* **10**, 2041-2056 (1977).
- <sup>33</sup>L. A. Crum, *Nature* **278**, 148-149 (1979).